pH-controlled breakup of fractal aggregates, microgels and gels formed by self-assembled amphiphilic triblock copolymers

Gireeshkumar Balakrishnan, Marli Miriam De Souza Lima, Frederick Niepceron, Olivier Colombani, Taco Nicolai, Christophe Chassenieux

ARTICLE

pH-Controlled Breakup of Fractal Aggregates, Microgels and Gels formed by Self-Assembled Amphiphilic Triblock Copolymers

Received 00th January 20xx,
Accepted 00th January 20xx

DOI: 10.1039/x0xx00000x

Gireeshkumar Balakrishnan Nair[a], Marli Miriam De Souza Lima [a,b], Frederick Niepceron [a], Olivier Colombani [a], Taco Nicolai [a*] and Christophe Chassenieux [a*]

The degradation of (micro)gels and fractal aggregates based on self-assembled amphiphilic triblock copolymers has been investigated in water by confocal microscopy and light scattering respectively. The triblock copolymer consisted of a central hydrophilic poly(acrylic acid) (pAA) block and two hydrophobic end blocks that contained an equal amount of randomly distributed n-butyl acrylate (nBA) and AA units. These latter units helped at tempering the hydrophobic end blocks resulting in the control and the fine tuning of the dynamics of the self-assembled triblock through the pH. Starting from a pH where the dynamics is frozen, the rate of breakup of the macroscopic gels, microgels and of fractal aggregates was measured after increasing the pH to different values. The mechanism of the breakup was found to be independent of the pH, but its rate increased exponentially with increasing pH. The degradation proceeded through the release of the polymers from the bulk into the surrounding aqueous phase.

Introduction

Hydrogels are soft material that can embed up to 95% of water within a network whose crosslinks can be covalent, physical or of both types. If hydrogels are used for the delivery/release of active molecules[1] or for other bio-related applications for which long-term stability may be a key issue[2], it is important to control and predict their degradation pattern either in terms of kinetics or ultimate degradation time. Two different mechanisms have been observed, namely bulk and surface degradation (or a combination of the two) depending on the type, density and distribution of the degradable moieties of the hydrogels[3] and have been mostly investigated by measuring mass loss and rheological properties upon degradation.

For chemical hydrogels, the control of the degradation pattern may be achieved through the incorporation of specific cleavable sites within the hydrogels during their synthesis[4]. This method has been well documented for so-called tetra-PEG (polyethylene glycol) hydrogels that are bio-compatible and form ideal networks whose degradation time can be varied widely without affecting their elastic modulus and water content[2]. These chemical hydrogels are based on four-armed star-like PEG chains bearing functional moieties at each end that can be further cleaved upon exposure to enzymes[1] or light[5] or by hydrolysis[6, 7]. The orientation of the degradation mechanism from bulk to surface is mainly driven by the location of the cleavable sites and by the crosslink density and network connectivity[5]. By extending the PEG chains with short hydroxyl acid segments of various hydrophobicity, Moeinzadeh et al. [7] have shown that the degradation was faster with decreasing hydrophobicity. For the less hydrophobic cleavable group, they have also reported a shift of the degradation mechanism from bulk to surface when decreasing the polymerization degree of the hydroxy acid group, which was attributed to a better ability to form hydrophobic crosslinks with longer blocks.

Simulation of the degradation of such gels has been achieved by modelling the bond breaking as a stochastic process utilizing Dissipative Particle Dynamics. The model shows that the degradation follows first order kinetics[8], which captures quite well the experimental results[2]. The mass loss is initially slow and takes place at the surface followed by bulk degradation of the network, which causes a faster mass loss. Less ideal chemical networks containing loops and dangling ends have also been investigated both experimentallly[9] and by modeling[10]. Degradation patterns are more complex in this case, because the number of elastically active chains that are lost during the degradation are not directly proportional to the number of cross-links. When dealing with chemical microgels, cleavable sites may also be engaged to control their degradation kinetics[11-13].

The degradation of physical hydrogels is achieved by taking advantage of the reversible nature of the crosslinks that may break after dilution or modification of the environment when

[a] Institut des Molécules et Matériaux du Mans, IMMM - UMR 6283 CNRS, Le Mans Université, Avenue Olivier Messiaen, 72085 LE MANS CEDEX 9, France
[b] Laboratório de Fitoquímica e Desenvolvimento Tecnológico - LAFITEC, Departamento de Farmacia - DFA, Universidade Estadual de Maringá-UEM, Maringa, Paraná, Brasil.

† Footnotes relating to the title and/or authors should appear here.

Electronic Supplementary Information (ESI) available: [details of any supplementary information available should be included here]. See DOI: 10.1039/x0xx00000x

dealing with so-called "smart materials". Tae et al.[14] have investigated in depth the degradation of physical hydrogels formed by self-assembly of triblock copolymers with a central hydrophilic block based on PEG capped with hydrophobic fluorinated alkyl chains at both ends. The hydrophobic groups assemble in aqueous solution and form flower like micelles that increasingly bridge between each other with increasing concentration. The exchange time of the hydrophobic blocks between micelles can be varied by varying the length of the fluorinated hydrophobic blocks. For short ones, the exchange time is small and the aggregates percolated to form a homogeneous system spanning network. For longer hydrophobic blocks, phase separation occurred between a dense gel phase and a liquid phase with a low polymer concentration. The degradation of both types of gels has been investigated by placing them in a reservoir filled with water. The degradation of homogeneous physical gels upon dilution was very fast and proceeded through bulk degradation and release of micelles. The degradation of phase separated physical gels was much slower due to the longer life time of the bridges between micelles and occurred at the surface of the gel. The degradation rate reflected the exchange time of the hydrophobic groups and correlated with the viscoelastic relaxation time of the gels.

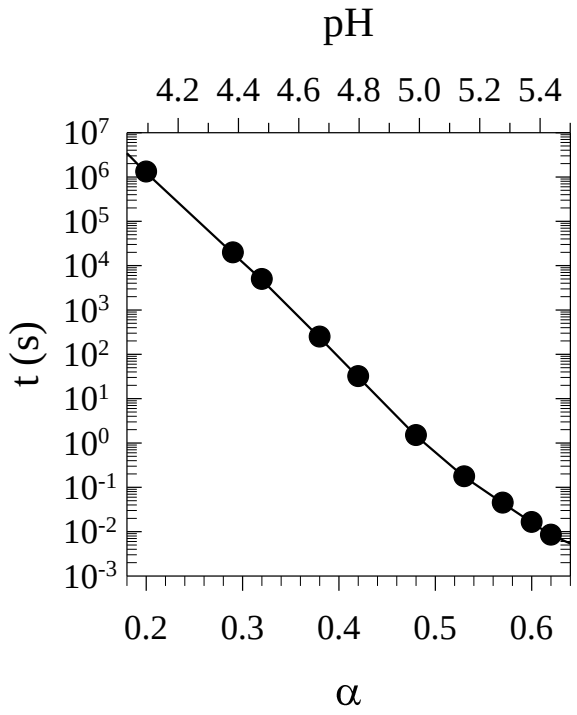

Figure 1 : Variation of the terminal viscoelastic relaxation time measured above the percolation concentration as a function of the ionization degree/pH (α/pH) for hydrogels based on an amphiphilic triblock named TH50 composed of a central poly(acrylic acid) block end-capped with two hydrophobic block based on poly(butyl acrylate) where 50mol% of acrylic acid units have been randomly incorporated (see the experimental section for details about the structure and the polymerization degrees of each block). TH50 results have been compiled from refs[15, 16]. The pH window has been restricted to the values investigated in the current article. The line is a guide for the eyes.

In the past, we have reported on the possibility to tune the viscoelastic relaxation time from milliseconds up to years for physical hydrogels obtained by the self-assembly of pH sensitive triblock copolymers[15, 17]. These copolymers consist of a central hydrophilic block made of poly(acrylic acid) (pAA) end-capped with two hydrophobic blocks containing both hydrophilic AA and hydrophobic n-butyl acrylate (nBA) units randomly distributed. In aqueous solution the hydrophobic end-blocks self-assemble into flower-like micelles at low concentrations. As for the system investigated by Tae et al.[14], larger aggregates are formed by bridging of the micelles with increasing concentration until a system spanning network is formed above a percolation concentration (Cp). An important difference is, however, that for pAA based systems, homogeneous gels were formed irrespective of the lifetime of the bridges possibly because the polymers were charged. If the end-blocks contained only hydrophobic nBA units, the association was irreversible as the activation barrier for the end-blocks to escape from the micellar core is very high[18]. By incorporating pH-sensitive hydrophilic AA units in the end-blocks the escape time was reduced and the association became dynamic. As a consequence, the system became a viscoelastic solution with a terminal relaxation time that was determined by the lifetime of the cross-links. Interestingly, the latter was found to strongly increase with decreasing pH, see fig. 1, which can be explained by the corresponding decrease of the degree of ionization of the AA units (α) and consequently the increased hydrophobicity of the end-blocks[15]. The pH-window where the gels transition from frozen to dynamic depends on the chemical composition of the triblock copolymers[17].This possibility to fine tune the life time of crosslinks from immeasurably long to very short by changing the pH has been exploited in the current study to investigate the effect of crosslink dynamics on the degradation kinetics of hydrogels.

At low pH, the rate of dissociation becomes so slow that the association can be considered irreversible on time scales of the experiment. Therefore, the morphology of the systems can be frozen by reducing the pH. In order to ensure that the system was in equilibrium until the dynamics became frozen-in, the pH was decreased in-situ using D-glucono-δ-lactone (GDL), a lactone which progressively releases protons upon hydrolysis[16]. In this manner suspensions of fractal aggregates are obtained below Cp while a gel is obtained for C > Cp.

The objective of the present study is to investigate the breakup both of frozen fractal aggregates and gels when the pH is increased to different values. For this study we used triblock copolymers (TH50) which contained 50mol% AA units within the end-blocks whose polymerization degree is 100 while the central PAA block has a polymerization degree of 200. The life-time of the cross-links for these polymers in aqueous solution was found to increase exponentially with decreasing α for α<0.6 and the system behaved as a permanent hydrogel for α<0.2[16]. The corresponding pH-range where the behaviour changed from a free flowing liquid to a permanent hydrogel was from pH = 5.5 to pH = 4.4[15]. Here, we report on the monitoring by confocal laser scanning

microscopy (CLSM) and by light scattering of the breakup for (micro)gels and fractal aggregates obtained respectively above or below the percolation concentration. Starting from a state where the systems are frozen, we will show that their break-up upon increasing pH always occur in the same manner, the disruption speed being dependent on the final pH. The disruption speed is also closely related to the escape time of the tempered hydrophobic blocks within the hydrophobic core of the micellar junctions of the aggregates and (micro)gels. During the breakup of both the microgels and aggregates, the polymers are released mainly from bulk into the surrounding aqueous medium.

EXPERIMENTAL SECTION

1. Materials. A triblock copolyelectrolyte (TH50) : P(nBA50%-stat-AA50%)$_{100}$-b-PAA$_{200}$-b-P(nBA50%-stat-AA50%)$_{100}$ was synthesized as previously described[15]. Sodium hydroxide 1M (Lab-online), D-glucono-δ-lactone (GDL) (Fluka, ~99% of purity), sodium chloride (Lab-online, ~99% of purity), sodium phosphate monobasic (Sigma, ~99% of purity), sodium phosphate dibasic (Sigma, ~99% of purity), potassium dihydrogen orthophosphate (Fisher, ~99% of purity), phosphoric acid (Acros, ~99% of purity) were used as received.

2. Sample preparation. Solutions of TH50 were prepared at different concentrations in ultrapure water (Milli-Q) with the required amount of NaOH to achieve their full ionization. The solutions were filtered through 0.2µm pore size Acrodisc filters and NaCl was added to reach a total concentration of 0.5 M for Na^+ (for more details see[16, 19]). The required degree of ionisation (α=0.2) was reached by addition of D-glucono-δ-lactone (GDL), as previously described[16]. For the breakup studies at different pH a large excess (100 to 500 times of the original volume) was added of a phosphate buffer at the required pH containing 0.2 M of phosphates and 0.3 M NaCl. It was verified that the sample had the required pH after addition of the buffer. The relationship between the pH and α for this system was reported elsewhere[20] for corresponding diblock copolymers that formed individual micelles. We verified that the same relation was obtained for TH50 that formed a network. The buffer solution was filtered through 0.1µm pore size Acrodisc filters prior to use. Two types of samples were prepared. The ones prepared above the percolation concentration (C_p=12g/L, see fig. 7b) and that formed gels, whereas samples at lower concentrations formed suspensions of fractal aggregates. Note that the ionic strength at which gels and aggregates were prepared matched the ionic strength of the buffers.

3. Methods. Light scattering measurements were done with an ALV-CGS3 system operating with a vertically polarized laser with wavelength λ=632nm. The measurements were done at 20°C controlled by a thermostat bath to within ±0.1°C, over a range of scattering wave vectors ($q=4\pi.n.\sin(\theta/2)/\lambda$), where θ is the angle of observation and n is the refractive index of the solvent. The relative scattering intensity (I_r) was calculated by subtracting, the solvent scattering intensity from the solution scattering intensity and normalizing by the scattering intensity of toluene. In diluted solutions I_r is related to the weight average molar mass (M_w) and the z-average structure factor S(q)[21]:

$$I_r=K.C.M_w.S(q) \quad (1)$$

with C the solute concentration and K an optical constant defined as:

$$K=4\pi^2 n_s^2 (dn/dC)^2/(\lambda^4 N_a R_\theta) \quad (2)$$

where N_a is Avogadro's number, dn/dC is the specific refractive index increment of the solute, R_θ is the Rayleigh ratio of toluene and n_s its refractive index. The refractive index increment was determined as dn/dC=0.15 mL/g [19]. In dilute solution the initial q-dependence of S(q) can be used to determine the z-average radius of gyration (R_g) of the solute:

$$S(q)=1/(1+(q^2.R_g^2)/3) \text{ when } qR_g<1 \quad (3)$$

Confocal laser scanning microscopy (CLSM) images were obtained with a Zeiss LSM800 CLSM microscope (Carl Zeiss Microscopy GmbH, Germany). Images of 512x512 pixels were produced using different water immersion objectives (HCXPL APO 63X NA=1.2 and 20X NA=0.7). The polymers were visualized by adding 5 ppm of rhodamine B that bound spontaneously to the polymers at all pH within the investigated range. The CLSM images were processed using the Image J software.

RESULTS AND DISCUSSION

Macroscopic gels were prepared at C=30g/L and α=0.2 (pH 4.1), where the exchange dynamics is immeasurably long, in wells (8x8 mm) that could be used directly for observation with confocal microscopy. The height of the gels was approximately 0.3 mm. Buffers of various composition were put on top of the gels in order to reach various final pH values. Microgels were formed by mechanically breaking macroscopic gels into small pieces with a range of sizes. The microgels were subsequently suspended in excess buffer at different pH. Large fractal aggregates were prepared by lowering the charge density of polymers to α=0.2 in solutions below the percolation concentration . The fractal aggregates were subsequently dispersed in excess buffer at different pH. In the following we will discuss first the break-up of macroscopic gels, then of microgels and finally of fractal aggregates. For macrogels, the release of polymers from the gel into the surrounding liquid could only occur from one side, whereas the microgels and fractal aggregates were completely surrounded with solvent.

Breakup of macroscopic gels

Figure 2 displays intensity profiles of macrogels as a function of the height that were recorded for two final pH values corresponding to two limiting situations. Figure 2a shows the

results for a gel after increasing the pH from 4.1 to 4.4. The square profile of the gel remained the same from the start up to 60 hours implying that no swelling nor disruption of the gel through release of materials to the buffer occurred during that time. The pH increase leads to a decrease of the hydrophobicity of the end blocks which leads to a decrease of their viscoelastic relaxation time by 2 orders of magnitude, see figure. 1. However, the decrease of the escape time of the hydrophobic blocks is not large enough at pH 4.4 to allow release of the triblock copolymers from the gel to the surrounding water.

The situation is different after increasing the pH to 5.4. In this case the initial square profile is lost after 60 minutes and takes the shape of a reverse sigmoid, see figure 2b. Upon increasing time, the inverted S profile flattens, its width increases and the intensity at the higher heights increases. This result can be understood by the release of polymers from the gels into the surrounding water until a homogeneous polymer solution is obtained at equilibrium. The release at pH = 5.4 can be understood from the fact that the exchange dynamics becomes faster when the pH is increased as reflected by a decrease of the viscoelastic relaxation time by almost 8 orders of magnitude between pH 4.2 up to pH 5.4, see figure 1.

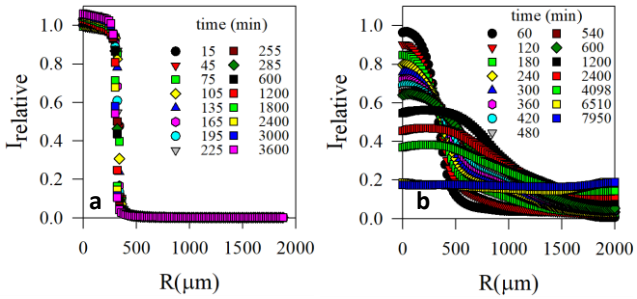

Figure 2 : Time evolution of the intensity profiles of TH50 gels marked with rhodamine B, prepared at pH 4.1 and covered by buffers with pH 4.4 (a) and 5.4 (b) as a function of the height (R). The intensity was normalized by the value at R = 0 before adding buffer. The times in minutes are indicated in the legend, for clarity not all the measurements are shown.

To better quantify the influence of the final pH on the disruption of the gels prepared at pH 4.1, we have monitored the relative fluorescence intensity at R = 0 as a function of time for different final pH (figure 3a). At pH 4.4, the intensity remained constant for hours, because there was no release of material from the gel towards the surrounding aqueous phase. When the final pH was increased, the intensity decreased faster and increasingly with increasing pH. Interestingly, all the data superimpose onto a master curve after normalizing the intensity by its initial value and the time by a characteristic time (tc) to reduce the intensity by 20% (Figure 3b). This means that the disruption of the gels proceeded in the same way, but at rates that depend on the pH. tc was much longer than the terminal relaxation time measured by rheology and shown in figure 1, which roughly corresponds to the characteristic escape time of the hydrophobic blocks[22]. This is expected, because the hydrophobic blocks that have escaped can easily enter into another micellar core. Therefore, many escapes are needed before the polymer is released to the surrounding aqueous phase. We note that the relative decrease of tc with increasing pH, in the narrow range where it could be measured, was less steep (almost 1 decade from pH 4.9 to 5.4, see figure 3b) than that of the relaxation time (~ 2.5 decades, see figure 1). This means that although the increasing breakup rate of the gel is clearly caused by a decrease of the bond lifetime, it is not proportional to the latter. Notice that a different definition of tc leads to different absolute values, but the same dependence on the pH.

Breakup of microgels

CLSM images of microgels are shown in fig. 4 as a function of time after adding excess buffer at different pH. For pH ≤ 5.0 the microgels remained intact for the whole period, but the fluorescence intensity varied with time. However, at higher pH the microgels completely melted after a relatively short time that decreased with increasing pH.

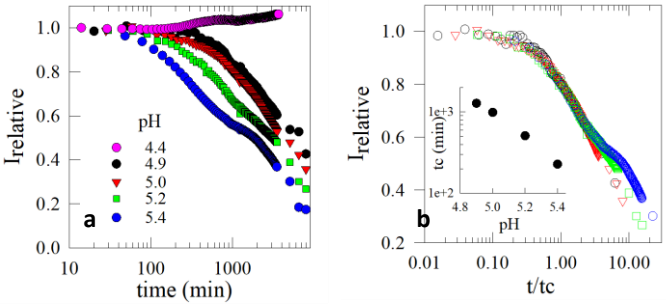

Figure 3 : Time evolution of the fluorescence intensity in the plane at R= 0 at various final pH indicated in the legend (a). The master curve of the same data has been obtained by normalizing time by tc when the intensity is reduced by 20% (b), with tc as a function of the pH shown in the inset.

Subsequently, a more or less homogeneous layer was formed that clarified slowly as the polymers dispersed in the medium. The relative change of the fluorescence intensity was measured as a function of time for selected areas within individual microgel particles. For a given system, the time dependence of the fluorescence intensity observed for different areas within the same microgel or within other microgels of different sizes was the same.

The fluorescence intensity as a function of time after setting the pH at different values has been measured for different microgels and its average is shown in figure 5. At pH 4.6 no change was observed within 15 h and at a lower pH of 4.0 the intensity even increased initially by about 30%. This increase can be explained by the fact that at pH 4.0 the microgels shrank a little, see fig. 4. We believe that this shrinkage was caused by the reduction of the charge on the polymers when the pH was decreased. At pH 4.9 and 5.0, the size of the microgels did not change significantly, but the intensity decreased progressively. At pH 5.1 the intensity decreased initially progressively as at pH 5.0, albeit faster, but after about 350 min the intensity decreased more steeply with time. Similar behaviour was found at higher pH at a rate that increased with increasing pH. The images show that the microgels started to melt before the intensity started to decrease more sharply. These observations suggest that during

the breakup process of microgels, polymers progressively escape from the microgels reducing the density of the polymer network. Considering that the bond lifetime was many orders of magnitude shorter, it is clear that the escape involved many instances of bridge breaking and reformation. At some point, the microgels fall apart (melt) into smaller clusters that continue to disintegrate into individual chains that diffuse away. It was not possible to obtain a master curve of the decrease of the intensity by pH-time superposition.

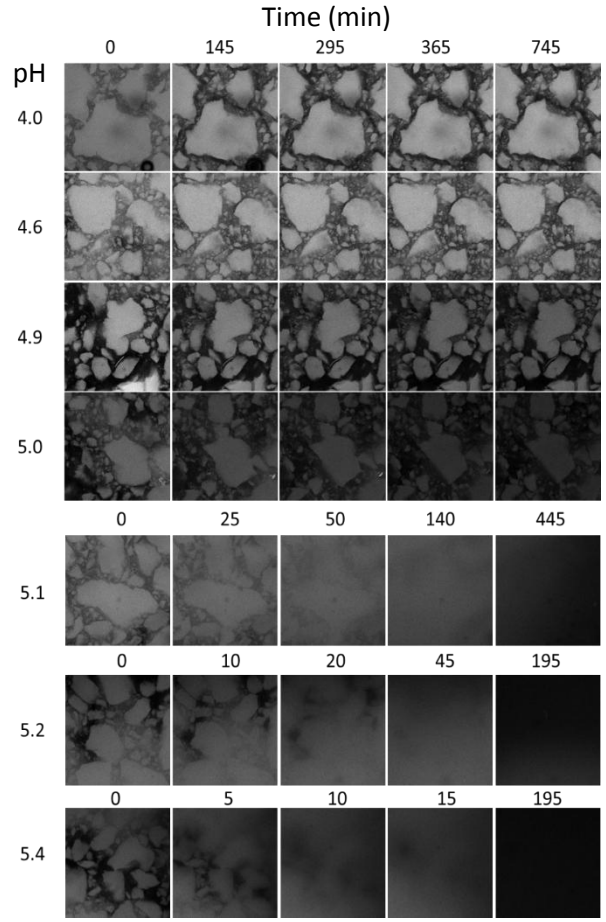

Figure 4 : CLSM images of microgels at different times in minutes after setting the pH to different values as indicated in the figure. The size of an image is 500x500µm.

Therefore, it is difficult to quantitatively characterize the rate of breakup as a function of the pH. Nevertheless, it is clear that the rate at which the microgels broke up increased very strongly with increasing pH suggesting that it is also controlled by the bond lifetime.

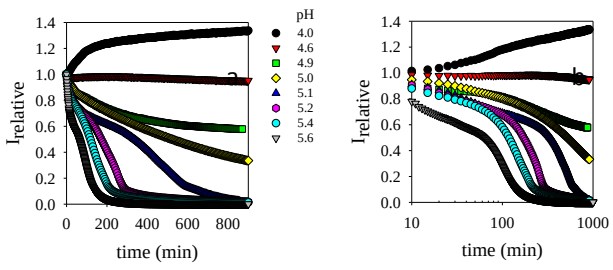

Figure 5 : Variation of the fluorescence intensity as a function of time on a linear (a) and logarithmic (b) scale after setting the pH to different values as indicated in the figure.

The degradation of the gels with short bond lifetimes resemble that reported by Tae et al.[14] for self-assembled neutral triblock copolymers. However, the results obtained at long bond lifetimes were different as for the neutral system surface erosion was observed. This can be explained by the fact that in the neutral system the bridged micelles phase separated forming a densely cross-linked gel so that when this system was put in excess water, polymers could only escape from the surface of the phase separated gel.

Breakup of fractal aggregates

Aggregates formed at different concentrations between 5 and 12 g/L at α=0.2 were stable to dilution which enabled characterization by light scattering. The scattering wave vector (q) dependence of $I_r/(KC)$ for aggregates formed at different concentrations is shown in fig. 6a.

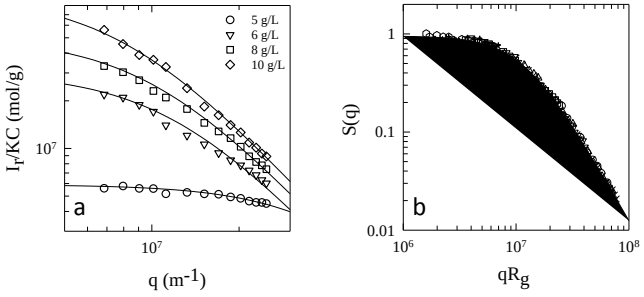

Figure 6 : a) q-dependence of Ir/KC for aggregates formed by self-assembly of TH50 at different concentrations as indicated in the legend of the figure at α=0.2. The solid lines represent fits to eq. 1 using eq.3 for S(q). b) Structure factor of the aggregates formed at different concentrations as a function of $q.R_g$. The solid line represents eq. 3. Results for all aggregates studied are shown in fig. 6b, but for clarity fewer are shown in fig. 6a

The value extrapolated to q=0 corresponds to the weight average molar mass of the aggregates ($M_{w,agg}$) and $I_r/(KCM_{w,agg})$ is equal to the structure factor S(q), see eq. 1. It was found that in all cases the structure factor could be well described by eq. 3 over the whole q-range, which allowed us to determine the z-average radius of gyration (R_g). The structure factors of aggregates formed at different concentrations superimposed when plotted as a function of $q.R_g$, see fig. 6b. At qR_g>>1, S(q) has a power law dependence on q implying that the aggregates were self-similar: $S(q) \propto q^{-df}$ where d_f is the so-called fractal dimension of the aggregates. In the present case we found that d_f=2.0.

Figure 7a shows that, as expected for fractal aggregates, the radius of gyration and the hydrodynamic radius increased with the molar mass following a power law dependence: $M_{w,agg} \propto R^{df}$. The value of d_f obtained in this way was consistent with that derived independently from S(q). In figure 7b the molar mass of the aggregates is plotted as a function of the concentration at which the aggregates were formed. $M_{w,agg}$ increased with increasing concentration and diverged at the

percolation concentration (C_p = 12 g/L) beyond which a system spanning network was formed.

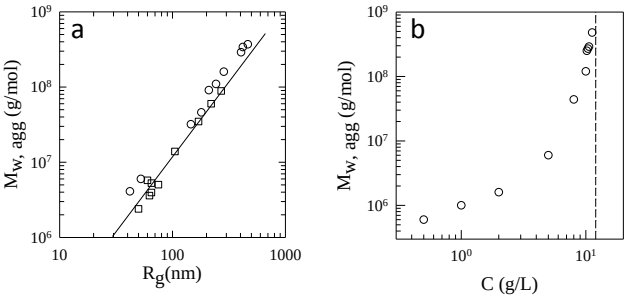

Figure 7 : a) Dependence of the molar mass on the radius of gyration for fractal aggregates formed by self-assembly of TH50 at different concentrations at α=0.2 (pH 4.1) (circles) or during breakup of the aggregates after setting the pH at 4.8 (α=0.4) (squares). The solid lines have slope 2. b) Molar mass of fractal aggregates as a function of the preparation concentration of TH50 at α=0.2 and with a total Na^+ concentration of 0.5 M. The dashed line indicates the percolation concentration.

The results obtained here for triblock copolyelectrolytes are similar to those obtained with neutral triblock copolymers[23]. In the latter case the dynamic self-assembled aggregates were frozen-in by in-situ photo crosslinking of the hydrophobic cores. It was shown that the concentration dependence of the molar masses of those aggregates agrees well with computer simulations of reversibly aggregating spheres indicating that bridging flower-like micelles can be modelled as sticky spheres. In order to study the kinetics of the breakup of fractal aggregates with a given bond lifetime, large fractal aggregates with $M_{w,agg}=10^8$g/mol were prepared (C=10g/L and α=0.2). Subsequently, they were highly diluted in a buffer solution with chosen pH values in the range 4.3 to 5.4 corresponding to ionization degrees between 0.25 and 0.6. In this range α increases approximately linearly with the pH. We showed elsewhere[16] that after increasing α the viscoelastic relaxation time reaches its steady state value within seconds. This allowed us to determine the kinetics of the breakup of fractal aggregates with a fixed bond lifetime after dilution in the buffer.

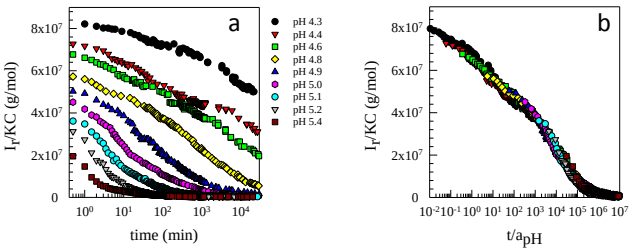

Figure 8 : Time dependence of I_r/KC for a solution of fractal aggregates prepared at 10g/L and α=0.2 (pH=4.1) after dilution into phosphate buffers at different pH indicated in the figure (a) and the corresponding master curves obtained by time-pH superposition with reference pH=4.8 (b).

The evolution of I_r/KC with time at a fixed scattering angle (30°, q = 7×10^6 m^{-1}) was monitored for a period up to a month after dilution, see figure 8a. Note that at this angle of observation, I_r/KC < $M_{w,\,agg}$ for larger aggregates for which q.R_g is not much smaller than 1. At pH 4.3 the decrease of the scattering intensity was less than a factor of two after a month while at pH 5.4 the aggregates were almost completely disrupted into individual flower-like micelles during mixing with the buffer (results not shown). A master curve was obtained if the times at different pH were divided by a factor a_{pH} so that the data overlapped with those at pH 4.8, see figure 8b, which suggests that the breakup occurred by the same mechanism at different pH, but at various rates. The decrease of the intensity is approximately exponential with time.

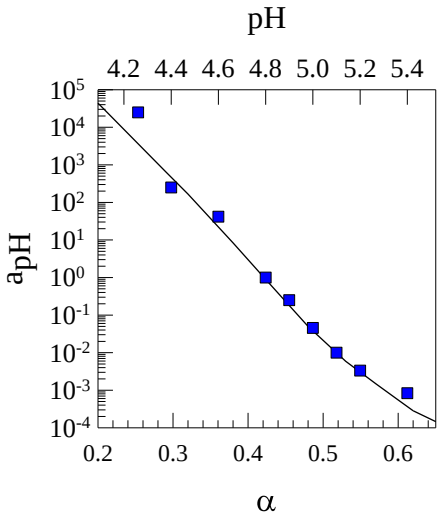

Figure 9 : Comparison of the pH dependence of the break down kinetics (blue squares) of fractal aggregates with that of the terminal relaxation time of the shear modulus of transient networks (solid line) taken from ref [15, 16]. The reference pH is 4.8.

The pH dependence of the shift factors (a_{pH}) corresponds to the relative variation of the decay time as a function of the pH. In figure 9, we compare the pH-dependence of the breakup kinetics in terms of a_{pH} with that of the terminal relaxation time (τ) of the shear modulus of transient networks formed at C>C_p that were reported in ref.[15, 16] , see fig. 1. It is clear that the rate of break-up has the same pH dependence as the mechanical relaxation time, which implies that both are controlled by the escape time of the end-blocks. However, the time needed to break-up the aggregates accessible through scattering experiments is orders of magnitude longer that the escape time of a single end-block that is measured by rheology, which is only about 10s at pH 4.8. The reason is that neighbouring micelles are connected by several bridges that all need to break at the same time in order to break the connection between two micelles. In addition, connections between micelles can be reformed if they remain close to each other as we mentioned above to explain the much slower breakup of macroscopic gels. This explains why the breakup process of the aggregates extends over many decades in time. Interestingly, we find that the pH dependence of the rate of breakup of fractal aggregates is nevertheless proportional to that of the bond lifetime, whereas the breakup rate of the macrogels depended less steeply on the pH.

In order to obtain more details about the structure of the aggregates during the breakup process, we determined the structure factor as a function of time after setting the pH to 4.8. At this pH, breakup is sufficiently slow to allow scanning of the scattering intensity over a range of angles, see Fig. S1a of the supplementary information. A master curve could be obtained and the structure factor could be well described by eq. 3 see Fig. S1b of the supplementary information, which means that the self-similar structure persisted during breakup. This is expected if we consider that during breakup of the aggregates, bridges between the micellar core are constantly broken and reformed in the same manner as during formation of the aggregates. Within the experimental error, the radius of gyration showed the same power law dependence on M_w as for the frozen aggregates formed at different C, see figure 7a, though R_g was systematically about 30% larger for a given molar mass. The latter indicates that the aggregates swelled when the charge density of the polymers was increased by increasing the pH. Since in this case the q-dependence was measured, M_w could be determined even for the large aggregates, which allowed us to confirm that it decreased logarithmically with time, see fig. S2 of the supplementary information.

Conclusions

Self-assembled fractal aggregates, microgels and gels of bridged micelles can be formed by pH sensitive triblock copolymers consisting of a central hydrophilic block and lateral tempered hydrophobic blocks. Starting from a frozen state, the self-assemblies can subsequently be broken up in a controlled manner at a rate that can be varied by many orders of magnitude by varying the pH. The fractal aggregates break up progressively into smaller aggregates with the same fractal structure. The microgels remain initially largely intact, but progressively release polymers from their interior at a rate that increased rapidly with increasing pH. When the density of the microgels has decreased to a critical value, they break up and subsequently disperse. For macroscopic gels, the same conclusions can be drawn though the release of polymeric material only occurs from one side. In all cases, the break up time is clearly controlled by the escape time of the tempered blocks from the physical cross-links of the network and that can be easily determined by rheology. Breakup is orders of magnitude slower than the escape time of a single hydrophobic block, because disconnecting two neighbouring micelles involves concomitant escape of several hydrophobic blocks. Furthermore, a fine control of the dynamics of exchange of the system may be achieved either by controlling its chemistry or through the mixing of polymers with various composition[24] which will help at shifting the pH window where the disruption of the gels will proceed.

Author Contributions

GBN, MMSL and FN Investigation and Vizualization. OC Writing, review and editing. TN Conceptualization, Vizualization, Methodology, Writing-Original draft, Writing-Review and Editing. CC Investigation, Funding acquisition, Conceptualization, Supervision, Writing-Original draft, Writing-Review and Editing.

Conflicts of interest

"There are no conflicts to declare".

Acknowledgements

The authors acknowledge the financial support of the French Agence Nationale de la Recherche in the frame of the MACAOS project (ANR-18-CE06-0015). The authors also thank "plateforme Matière Molle of IMMM" where all the experiments have been carried on.

References

1. N. Wu and K. M. Schultz, *Biomacromolecules*, 2021, **22**, 4489-4500.
2. X. Li, S. Kondo, U.-I. Chung and T. Sakai, *Chemistry of Materials*, 2014, **26**, 5352-5357.
3. P. M. Kharkar, K. L. Kiick and A. M. Kloxin, *Chemical Society Reviews*, 2013, **42**, 7335-7372.
4. H. L. Lim, Y. Hwang, M. Kar and S. Varghese, *Biomaterials Science*, 2014, **2**, 603-618.
5. M. W. Tibbitt, A. M. Kloxin, L. A. Sawicki and K. S. Anseth, *Macromolecules*, 2013, **46**, 2785-2792.
6. E. Jain, L. Hill, E. Canning, S. A. Sell and S. P. Zustiak, *Journal of Materials Chemistry B*, 2017, **5**, 2679-2691.
7. S. Moeinzadeh, D. Barati, S. K. Sarvestani, O. Karaman and E. Jabbari, *Biomacromolecules*, 2013, **14**, 2917-2928.
8. V. Palkar, C. K. Choudhury and O. Kuksenok, *MRS Advances*, 2020, **5**, 927-934.
9. T. K. L. Meyvis, S. C. De Smedt, J. Demeester and W. E. Hennink, *Macromolecules*, 2000, **33**, 4717-4725.
10. P. Martens, A. T. Metters, K. S. Anseth and C. N. Bowman, *The Journal of Physical Chemistry B*, 2001, **105**, 5131-5138.
11. G. Agrawal, J. Wang, B. Brüster, X. Zhu, M. Möller and A. Pich, *Soft Matter*, 2013, **9**, 5380-5390.
12. M. M. Coronel, K. E. Martin, M. D. Hunckler, P. Kalelkar, R. M. Shah and A. J. García, *Small*, 2022, **18**, 2106896.
13. H. Li, X. Li, P. Jain, H. Peng, K. Rahimi, S. Singh and A. Pich, *Biomacromolecules*, 2020, **21**, 4933-4944.
14. G. Tae, J. A. Kornfield, J. A. Hubbell, D. Johannsmann and T. E. Hogen-Esch, *Macromolecules*, 2001, **34**, 6409-6419.
15. C. Charbonneau, C. Chassenieux, O. Colombani and T. Nicolai, *Macromolecules*, 2011, **44**, 4487-4495.
16. C. Charbonneau, C. Chassenieux, O. Colombani and T. Nicolai, *Macromolecules*, 2012, **45**, 1025-1030.
17. A. Shedge, O. Colombani, T. Nicolai and C. Chassenieux, *Macromolecules*, 2014, **47**, 2439-2444.
18. E. Eghbali, O. Colombani, M. Drechsler, A. H. E. Müller and H. Hoffmann, *Langmuir*, 2006, **22**, 4766-4776.

19. C. Charbonneau, M. M. De Souza Lima, C. Chassenieux, O. Colombani and T. Nicolai, *Physical Chemistry Chemical Physics*, 2013, **15**, 3955-3964.
20. O. Colombani, E. Lejeune, C. Charbonneau, C. Chassenieux and T. Nicolai, *The Journal of Physical Chemistry B*, 2012, **116**, 7560-7565.
21. W. Brown, *Light Scattering: Principles and development*, Clarendon Press: Oxford, 1996.
22. T. Zinn, L. Willner and R. Lund, *ACS Macro Letters*, 2016, **5**, 1353-1356.
23. V. Kadam, T. Nicolai, E. Nicol and L. Benyahia, *Macromolecules*, 2011, **44**, 8225-8232.
24. L. Lauber, O. Colombani, T. Nicolai and C. Chassenieux, *Macromolecules*, 2016, **49**, 7469-7477.